

Article

Evaluation of Bioclimatic Discomfort Trend in a Central Area of the Mediterranean Sea

Pietro Monforte ^{1,2}  and Maria Alessandra Ragusa ^{1,*} ¹ Department of Mathematics and Computer Science, Catania University, 95124 Catania, Italy² I.R.S.S.A.T. Institute for Research, Development and Experimentation on the Environment and the Territory, 95033 Biancavilla, Italy

* Correspondence: mariaalessandra.ragusa@unict.it

Abstract: Effects of climate change are perceived in ever larger areas of the planet. Heat waves occur with increasing frequency, constituting a risk to the population, especially for the most sensitive subjects. Preventive information to the population on the characteristics of the phenomenon and on the behavior to be supported is the means to reduce the health risks. To monitor the intensity of heat and the physiological discomfort perceived by humans, there are indices based on the perception of meteorological parameters such as temperature and relative humidity. In this work, by applying the Thom Discomfort Index (TDI), the first bioclimatic characterization of the provinces that make up Sicily, a Mediterranean region defined as a hotspot for climate change, was performed by the authors. The nonparametric Mann–Kendall test was applied to the daily values of the TDI in all provinces in order to verify the presence of significant trends. The test results highlighted the existence of increasing trends, especially in the months of August and September, when the TDI value undergoes a significant increase due not only to high temperatures, as one might expect, but above all to a high humidity rate. When these two meteorological parameters reach certain values, the physiological discomfort from humid heat represents a risk to the population.

Keywords: climate change; heat wave; public health; bioclimatic discomfort; trend analysis; Mann–Kendall test



Citation: Monforte, P.; Ragusa, M.A. Evaluation of Bioclimatic Discomfort Trend in a Central Area of the Mediterranean Sea. *Climate* **2022**, *10*, 146. <https://doi.org/10.3390/cli10100146>

Academic Editor: Marco Delle Rose

Received: 13 September 2022

Accepted: 30 September 2022

Published: 5 October 2022

Publisher's Note: MDPI stays neutral with regard to jurisdictional claims in published maps and institutional affiliations.



Copyright: © 2022 by the authors. Licensee MDPI, Basel, Switzerland. This article is an open access article distributed under the terms and conditions of the Creative Commons Attribution (CC BY) license (<https://creativecommons.org/licenses/by/4.0/>).

1. Introduction

Nowadays in many areas of the planet, there are significant changes in climatic conditions [1–6]. Climate change and global warming are expected to significantly affect vulnerable areas such as the Mediterranean basin, with serious consequences [7,8].

Meehl and Tebaldi [9] have demonstrated that present-day heat waves over Europe and North America coincide with a specific atmospheric circulation pattern that is intensified by ongoing increases in greenhouse gases, indicating that it will produce more severe heat waves in those regions in the future.

One of the effects of these changes is the increase in heat waves, characterized by temperatures above the usual values [10–13]. Knowing how climatic and environmental factors can affect the health and well-being of the population is a current and important question, as evidenced by various studies conducted in Italy, Europe, the United States, and other parts of the world [14–17]. There is a common sensitivity to monitoring the effects of climatic and environmental conditions on human health, with the main goal of preventing and reducing risks to the population [18,19].

The heat wave is one of the factors linked to the climate, capable of causing hundreds of victims every year. Despite the widespread usage, intuitive understanding of the term “heat wave” and the associated impacts, there is no unified definition [20]. This is largely due to the multiple factors that will affect the character of a heat-wave event and that need to be clearly articulated. The World Meteorological Organization (WMO) has drafted guidelines on the definition and monitoring of extreme weather and climate events [21]. The

recommended definition of a heat wave is: “A period of marked unusual hot weather over a region persisting for at least three consecutive days during the warm period of the year based on local climatological conditions, with thermal conditions recorded above given thresholds.” Ebi et al. [22] proposed an approach for assessing human health vulnerability and public health interventions to adapt to climate change. Heat waves can be very tiring on the body even with a short period of exposure. Alonso and Renard [23] studied the physiological and socioeconomic vulnerabilities to heat waves in Lyon. Everyone can be vulnerable to heat waves, but some groups of individuals are at greater risk [24]. The highest-risk groups are elderly people (>75 years), particularly those with pre-existing diseases, people with cardiovascular and respiratory diseases, children, and infants, as their bodies have a reduced ability to adapt to heat compared to adults [25]. From this, it is clear that it is necessary to provide the population, and in particular the most sensitive subjects, with adequate information on the characteristics of the phenomenon and on the behaviors that make it possible to avoid the aggravation of any pathologies already present.

The development of procedures based on the complex dynamics with which air temperature, relative humidity, and wind are combined make it possible to identify the conditions of well-being or thermal discomfort felt by humans in hot periods. In this work, we used temperature and the relative humidity of the air as key parameters for the study of bioclimatic discomfort, because of their ability to alter the environment and cause bodily stress in the human population [26]. According to Masterton and Richardson [27], people react differently to the same temperature but different humidity levels.

In many European countries, including Italy, the summer of 2003 is particularly remembered, characterized by anomalous temperature values, among the highest in recent centuries, and long heat waves [28–31]. To protect the population from similar events, it becomes essential to identify when and in the presence of what weather conditions the state of health and well-being may be at risk. To monitor the intensity of heat and the resulting physiological discomfort in humans, there are various indices, all based on the perception of meteorological parameters such as temperature and relative humidity [32,33].

The aim of this work was to characterize from the prospective bioclimate the provinces that make up the island of Sicily, a Mediterranean region defined as a hotspot of climate change [34]. The characterization was conducted through the application of the Thom Discomfort Index (TDI) [35], one of the most reliable and used indices for the assessment of conditions of discomfort [36–39]. It is a daily index that expresses, through a single value, the effect of temperature and humidity in the form of a sensation of physiological discomfort perceived by the human body. The TDI was applied for a period of 20 years, from 2002 to 2021, considering only the hot months (May to September).

In order to verify the presence of significant trends, the nonparametric Mann–Kendall test (MKT) was applied to the daily values of the TDI in all provinces of Sicily [40,41]. Study of the time series of the TDI made it possible to identify the provinces most subject to bioclimatic discomfort. Analysis of the hot periods, in which public health is most exposed to risks, made it possible to identify the bioclimatic criticalities for each province. These criticalities are not to be underestimated, since in many European countries, including Italy [42], the population is aging. As a consequence, in the coming years, the percentage of the population susceptible to heat waves is expected to increase [43].

Given the impossibility of answering precise questions on the type of climate that will occur on Earth in the coming decades, the only possible solution at the moment is to focus on forecasting models. Knowing in advance that the heat wave is about to arrive makes it possible to optimally manage preventive interventions for the categories of subjects at risk.

2. Materials and Methods

2.1. Study Area

Sicily is the biggest island in the Mediterranean Sea, has a total area of about 25,000 km², and extends in latitude between about 36° and 38° north and in longitude between about 12° and 15° east. It is a predominantly hilly region—62% of the territory—24% is mountain-

ous and the remaining 14% is flat. Overall, the Sicilian orography shows sharp contrasts between the northern portion, mainly mountainous, the central-southern and southwestern portion, essentially hilly, the typical plateau, present in the southeastern area, and volcanic in the eastern part. From a climatic point of view, Sicily, according to the macroclimatic classification of Köppen, can be defined as a region with a temperate-humid climate of type C (average of the coldest month below 18 °C but above −3 °C). However, this definition has only a macroclimatic value, as on a regional scale the climate is strongly influenced by local factors, such as the conformation of the territory, the proximity to the coast, and the orography. According to [44,45], if we pass to the analysis of what can be found within the temperate climate of type C of Köppen, we can already distinguish several subtypes—temperate subtropical, temperate climate warm, sublittoral temperate, subcontinental temperate, and cool temperate—each of which can be found in the different areas of Sicily. The territorial diversity of Sicily consequently produces a complex climatic variability during the year in terms of temperature distribution and rainfall [46]. The administrative subdivision of Sicily is represented by nine provinces: Agrigento (AG), Caltanissetta (CL), Catania (CT), Enna (EN), Messina (ME), Palermo (PA), Ragusa (RG), Syracuse (SR), and Trapani (TP). Within each province, there are a variable number of municipalities, for a complex total of 390.

2.2. Data Sources

The weather data come from the Sicilian Agrometeorological Information Service (SIAS, <http://www.sias.regione.sicilia.it>, accessed on 1 December 2018). The detection network is made up of 96 weather stations located throughout the Sicilian territory since 2002, with good spatial coverage and temporal continuity. In this work, the data of average daily temperature and relative humidity acquired from 2002 to 2021 were used. For each year of data, only the hot months (May, June, July, August, September) were taken into account. For estimation of the missing daily values, the method of the mean difference was used, as recommended by the World Meteorological Organization [47]. This permitted us to obtain a continuous time series. Figure 1 shows the administrative subdivision of the island and the location of the weather stations.



Figure 1. Location of weather stations (red dots).

2.3. Thom Discomfort Index

The human body uses the evaporation of liquids present on the skin to cool itself. Evaporation occurs more effectively if the air is dry or slightly humid. If the air is very humid, the evaporation of sweat occurs with more difficulty: the heat is not dissipated and accumulates, causing feelings of discomfort and often heatstroke. The Thom Discomfort Index (TDI) describes physiological distress conditions caused by humid heat. The mea-

surement is calculated as the temperature and can be referred to the range 21 °C–47 °C. Beyond this range, the index always attributes “well-being” for temperature values below 21 °C and “medical emergency” for temperatures above 47 °C, regardless of the relative humidity value. The TDI combines in a single value the effect of temperature and humidity perceived by the human body, and is calculated using Equation (1):

$$TDI = T_m - 0.55 (1 - 0.01RH) (T_m - 14.5) \tag{1}$$

where T_m represents the average daily temperature (°C) and RH represents the daily relative humidity (%). As regards the conditions of physiological discomfort perceived by the population, six levels are identified [48,49], each representing a range of the TDI, as shown in Table 1.

Table 1. Thom’s discomfort conditions.

Range (°C)	TDI Class	Description
<21	I st	No discomfort
21–23.9	II nd	Under 50% of the population feels discomfort
24–26.9	III rd	Over 50% of the population feels discomfort
27–28.9	IV th	Most of the population suffers discomfort
29–31.9	V th	Everyone feels severe stress
>32	VI th	Medical emergency

By applying the TDI, it is possible to estimate the daily conditions of potential well-being and physiological discomfort. This provides extremely useful information on any health risks, especially when the persistence of uncomfortable heat conditions for the body occurs. It is generally more correct to speak of potential impact, as each individual responds differently to thermal stimuli. This response depends on a series of subjective factors, such as the thermoregulation system, age, the psychophysical characteristics of the subject, the type of activity carried out, the type of clothing worn, the duration of exposure, and the degree of acclimatization in the environment considered [50,51].

The TDI was applied for 20 years from 2002 to 2021, considering only the hot months (May to September). For each province, an average value of daily temperature and relative humidity was calculated, in order to calculate the daily value of the TDI that characterizes that part of the territory

2.4. Trend Analysis Method

In order to verify the presence of any trends, the Mann–Kendall test (MKT) was applied to the available time series. It is a nonparametric test; therefore, it does not assume any a priori distribution for the data. It allows to quantify the significance of trends in time series, and for this purpose it is often used for analysis of environmental time series [52–57].

In MKT, the null hypothesis (H_0) is that there is no trend in the observed series. The alternative hypothesis (H_A) is instead that the series follows a monotonous, increasing or decreasing, trend over time. The MKT statistic, denoted by S , is calculated using Equation (2):

$$S = \sum_{i=1}^{n-1} \sum_{j=i+1}^n \text{sgn}(x_j - x_i) \tag{2}$$

where x_j and x_i are, respectively, the values of the j -th year and i -th year, being $j > i$, n is the length of the series and the sign function. Equation (3), is defined as follows:

$$\text{sgn}(x_j - x_i) = \begin{cases} 1 & \text{if } x_j - x_i > 0 \\ 0 & \text{if } x_j - x_i = 0 \\ -1 & \text{if } x_j - x_i < 0 \end{cases} \tag{3}$$

If the series is sufficiently long ($n \geq 10$), the statistic S can be approximated to a normal distribution, Equation (4), with zero as average and variance equal to:

$$\text{Var}(S) = \frac{1}{18} \left[n(n-1)(2n+5) - \sum_{i=1}^g t_i(t_i-1)(2t_i+5) \right] \quad (4)$$

The second term is introduced to make the necessary correction in the presence of groups of equal observations that generate the so-called nodes, in particular g is the number of nodes and t_i is the number of nodes in the i -th group.

The statistics of the Z_s test are applied to calculate the significance of the trend. The Z_s test allows us to verify the null hypothesis H_0 . If $|Z_s|$ is bigger than $Z_{\frac{\alpha}{2}}$, where α represents the chosen level of significance (e.g., with $\alpha = 0.05$, $Z = 1.96$), then the null hypothesis is not true. This fact implies that the trend of the series is significant. The statistic Z_s is calculated as follows:

$$Z_s = \begin{cases} \frac{S-1}{\sqrt{\text{Var}(S)}} & \text{if } S > 0 \\ 0 & \text{if } S = 0 \\ \frac{S+1}{\sqrt{\text{Var}(S)}} & \text{if } S < 0 \end{cases} \quad (5)$$

where Z_s denotes the direction of the trend. We have an increasing trend if Z_s is positive, and a decreasing trend if Z_s is negative [58,59].

3. Results and Discussion

In this study, we characterized bioclimatic distress perceived in Sicily. It was decided to use the administrative subdivision of the territory, rather than considering the entire island, in order to obtain more detailed information. Using the daily data of temperature and relative humidity from the Sicilian Meteorological Service (SIAS), it was possible to calculate the Thom Discomfort Index (TDI) from 2002 to 2021 considering the months of May, June, July, August, and September for a total of 153 days per year.

To analyze the fluctuations in the TDI value, as a function of months and years, a contour plot for each province was created. In the function of the monthly and annual fluctuations of the TDI, it was possible to identify in which provinces exist the major critical issues that could cause physiological discomfort for humans.

As Figure 2 shows, the provinces behaved differently over the past two decades. Especially during the months of July and August, the TDI value undergoes a significant increase due not only to high temperatures, as one might expect, but above all to high humidity. When these two meteorological parameters reach certain values, the physiological discomfort due to humid heat represents a risk to the population.

In detail, in the provinces of EN and AG, the TDI values during the critical months do not reach such levels as causing physiological discomfort for humid heat. In the provinces of CL, ME, and PA, the TDI values from mid-June to the first days of September fluctuate between 21 and 24: "Under 50% population feels discomfort" (Table 1).

In the province of CT, the scenario changes, especially in the months of July and August, where TDI values fluctuate between 24 and 27, a range within which "Over 50% of the population feels discomfort." Worrying is what happens in the provinces of RG, SR and TP, since from mid-June to mid-September, the prevailing TDI values fluctuate between 24 and 27. Moreover, there are periods between 7 and 20 days in which the limit value of 27 is exceeded. This value corresponds to the IVth class of the TDI, in which "Most of the population suffers discomfort."

The development of the TDI as a time series has shown that during the warm period of the year in various provinces of Sicily, there are bioclimatic conditions capable of thermal stress on humans.

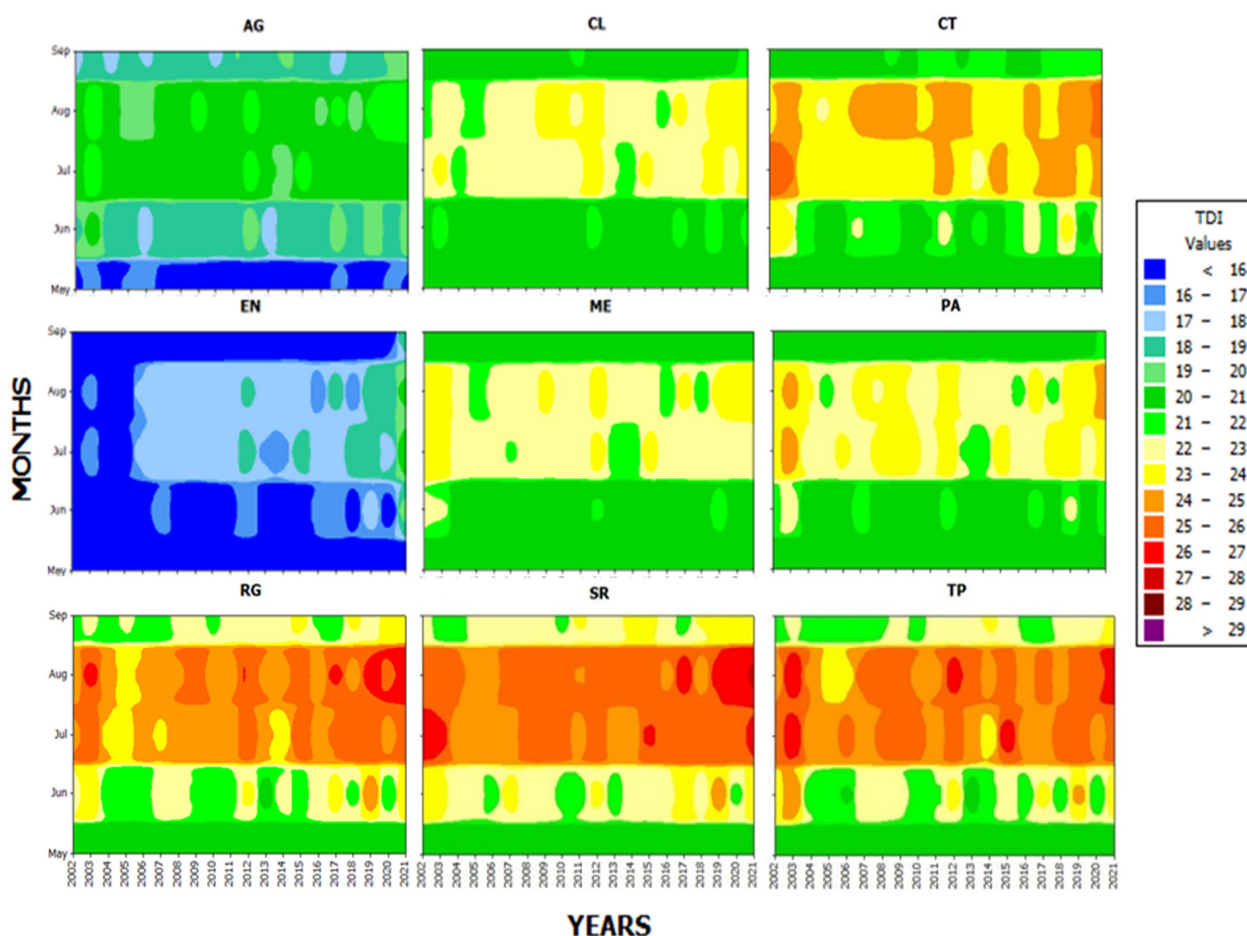


Figure 2. Contour plot of the TDI value as a function of the months and years of each province.

The statistical analysis conducted using MKT, with a significance level of 95%, made it possible to highlight in which provinces the growing trend of the TDI value occurs. In May, there is no trend in AG, CL, CT, or RG, while it is present in EN (increasing), ME (decreasing), PA (decreasing), SR (increasing), and TP (decreasing). In June, there is no trend in AG, CT, ME, PA, SR, or TP, while there is an increasing trend in RG, EN, and CL. In July, there is an increasing trend in CL, EN, RG, and SR, but no trend in AG, CT, ME, PA, or TP. In August there is no trend in PA, while in all the other provinces there is a growing trend. Finally, in September, a growing trend is identified in all the provinces. Table 2 shows the test results.

The annual distribution of days representing one of the six TDI classes was analyzed. A fact that unites all the provinces is the decreasing trend of the Ist class, which identifies the absence of discomfort. This implies an increase in the number of days representative of the worst classes.

The IInd class shows an increasing trend in six provinces (AG, CL, CT, EN, ME, PA), while it decreases in RG, SR, and TP. The scenario that emerges in these three provinces is not synonymous with an improvement in conditions: observing the IIIrd class, a greater slope of the regression line is noted, highlighting a rapid increase. In the provinces of CL and CT, the increase in class IIIrd is moderate. A different scenario can be observed in the provinces of ME and PA, where the trend of the IIIrd class shows a very slow decrease, while in the AG and EN provinces the IIIrd class is not present.

Class IVth is not present in the provinces of AG, CL, or EN; in ME and PA, the presence is rare, while in CT the presence, even if rare, is more incisive: in some years, it has approached 10 days. In the provinces of RG and SR, there is an increasing trend, while in TP the trend shows a slight decrease.

Table 2. Results of the Mann–Kendall test for TDI values in each province.

Prov.	Month	N° Obs.	Min	Max	Mean	Std. Dev.	Z _S	p-Value	Test Interpretation ($\alpha = 0.05$)	Trend
AG	May	620	10.76	20.78	15.64	1.66	−1.039	0.298	Accept H ₀	No Trend
	June	600	12.87	23.47	18.66	1.81	0.563	0.573	Accept H ₀	No Trend
	July	620	17.23	23.72	20.52	1.11	0.182	0.855	Accept H ₀	No Trend
	August	620	17.21	23.84	20.59	1.13	3.894	0.001	Reject H ₀	Increasing
	September	600	13.70	22.33	18.46	1.53	4.504	<0.001	Reject H ₀	Increasing
CL	May	620	10.96	23.17	16.81	2.02	0.937	0.348	Accept H ₀	No Trend
	June	600	12.95	25.25	20.33	2.15	1.967	0.041	Reject H ₀	Increasing
	July	620	18.47	26.11	22.64	1.29	3.341	0.008	Reject H ₀	Increasing
	August	620	18.03	25.82	22.67	1.33	6.381	<0.001	Reject H ₀	Increasing
	September	600	14.16	24.59	20.04	1.93	6.774	<0.001	Reject H ₀	Increasing
CT	May	620	10.57	23.77	17.49	2.27	−0.971	0.331	Accept H ₀	No Trend
	June	600	14.12	27.28	21.52	2.48	−0.008	0.993	Accept H ₀	No Trend
	July	620	19.55	28.38	23.96	1.55	0.214	0.830	Accept H ₀	No Trend
	August	620	19.46	28.36	24.08	1.49	2.985	0.002	Reject H ₀	Increasing
	September	600	15.12	26.21	20.95	2.14	3.719	0.002	Reject H ₀	Increasing
EN	May	620	8.38	18.45	12.84	1.79	8.012	<0.001	Reject H ₀	Increasing
	June	600	9.64	22.64	15.65	2.11	10.932	<0.001	Reject H ₀	Increasing
	July	620	11.68	22.36	17.36	1.64	15.791	<0.001	Reject H ₀	Increasing
	August	620	10.97	23.11	17.25	1.69	13.762	<0.001	Reject H ₀	Increasing
	September	600	10.22	21.08	14.99	1.86	12.561	<0.001	Reject H ₀	Increasing
ME	May	620	8.55	24.79	15.91	2.62	−2.672	0.007	Reject H ₀	Decreasing
	June	600	11.89	28.46	20.02	2.88	−1.231	0.218	Accept H ₀	No Trend
	July	620	17.35	29.26	22.48	1.86	−1.857	0.063	Accept H ₀	No Trend
	August	620	18.35	28.19	22.68	1.79	0.956	0.339	Reject H ₀	Increasing
	September	600	13.63	26.30	19.59	2.24	2.451	0.014	Reject H ₀	Increasing
PA	May	620	9.62	24.54	16.58	2.41	−2.131	0.033	Reject H ₀	Decreasing
	June	600	12.47	28.51	20.58	2.58	−0.789	0.423	Accept H ₀	No Trend
	July	620	17.88	28.61	22.97	1.61	−1.328	0.184	Accept H ₀	No Trend
	August	620	18.97	27.95	23.05	1.62	1.245	0.213	Accept H ₀	No Trend
	September	600	14.13	25.78	20.17	2.07	2.811	0.005	Reject H ₀	Increasing
RG	May	620	12.73	25.16	18.27	2.21	0.083	0.934	Accept H ₀	No Trend
	June	600	15.43	29.28	22.27	2.46	2.084	0.037	Reject H ₀	Increasing
	July	620	20.39	29.18	24.78	1.56	4.109	<0.001	Reject H ₀	Increasing
	August	620	20.55	29.49	25.12	1.55	6.832	<0.001	Reject H ₀	Increasing
	September	600	16.38	27.66	22.37	2.03	5.221	<0.001	Reject H ₀	Increasing
SR	May	620	12.71	24.23	18.45	2.06	2.938	0.003	Reject H ₀	Increasing
	June	600	16.15	28.47	22.69	2.37	1.787	0.074	Accept H ₀	No Trend
	July	600	16.64	27.81	22.53	2.01	2.649	0.008	Reject H ₀	Increasing
	August	620	20.96	29.41	25.51	1.41	4.929	<0.001	Reject H ₀	Increasing
	September	600	16.64	27.80	22.53	2.02	4.452	<0.001	Reject H ₀	Increasing
TP	May	620	11.32	25.51	18.24	2.24	−2.633	0.008	Reject H ₀	Decreasing
	June	600	14.57	28.83	22.34	2.51	−0.002	0.998	Accept H ₀	No Trend
	July	620	20.32	29.27	24.99	1.61	−0.039	0.968	Accept H ₀	No Trend
	August	620	20.79	30.12	25.17	1.65	3.255	0.001	Reject H ₀	Increasing
	September	600	15.88	27.72	22.21	2.11	3.622	0.001	Reject H ₀	Increasing

Regarding class Vth, it is very rarely present in RG, SR, or TP, while it is absent in all the others. Class VIth is not present in any of the provinces analyzed. The values of the analysis are shown in the Appendix A (Tables A1 and A2). Figure 3 shows the trends of the classes found in each province during the entire observation period.

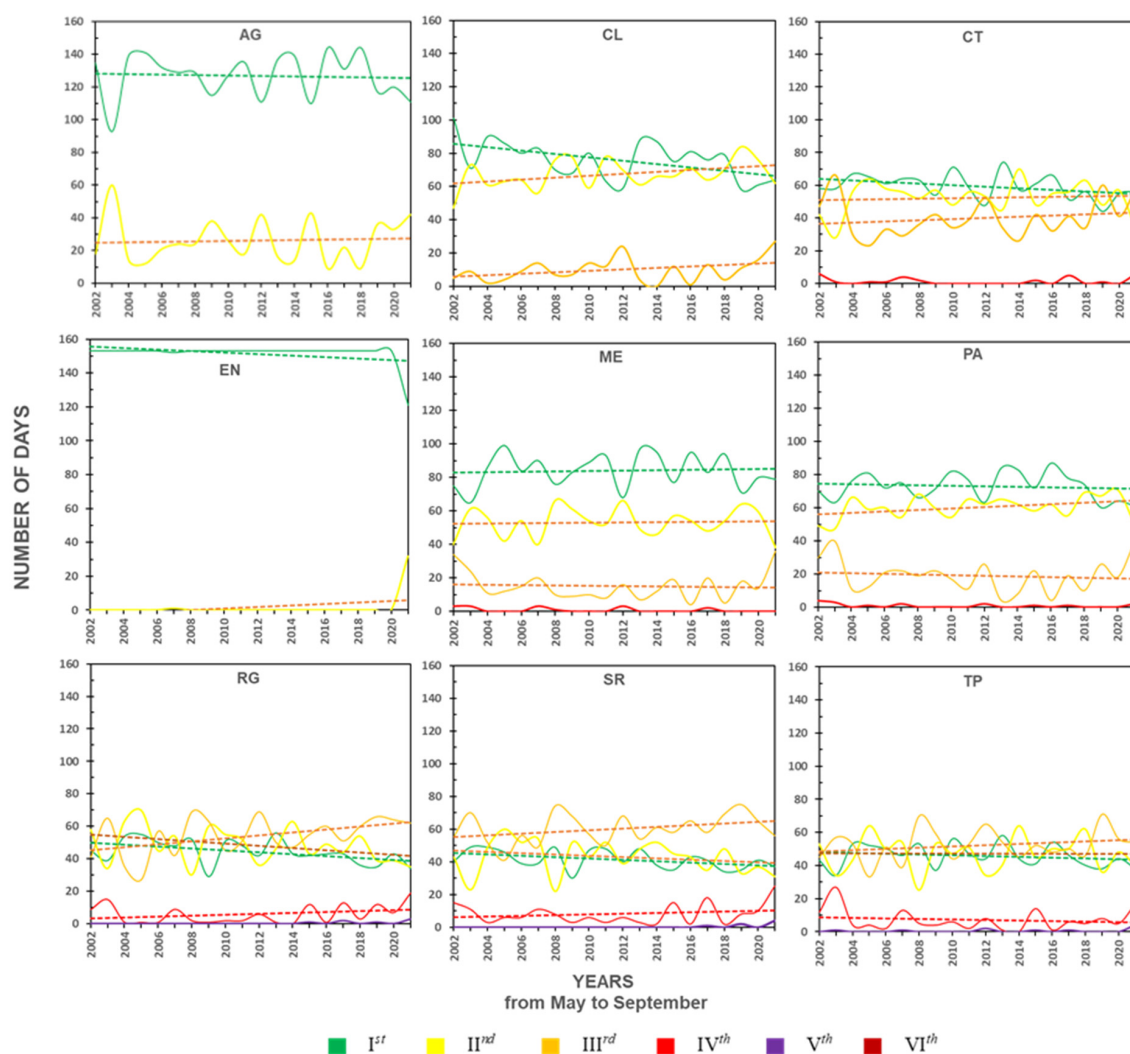


Figure 3. Trend of the number of representative days of each class from 2002 to 2021 (solid line) with regression line (dashed line).

By analyzing the time series of the TDI, it was possible to verify the presence or absence of trends, obtaining useful information for forecasting purposes.

The years with the highest TDI values were the last of the time period used, in accordance with the forecast of increased extreme heat events in the Mediterranean [60]. The index was also able to capture the fact that in the southern part of the island, the bioclimatic stress perceived by humans is greater than in the northern part.

Currently in Sicily, there are no studies dedicated to bioclimatic discomfort. This first study focused on the Sicily region differs from other works conducted in some Mediterranean regions [61,62]. This study analyzed the fluctuation of TDI over the past 20 years, highlighting the provinces most exposed to the health risk of heat waves.

It could be the starting point for the realization of a forecast model of the physiological distress perceived by the population. The results obtained by this model could be converted into information for the population about the climatic scenarios on the island during hot months.

The goal is to preventively reduce exposure to critical bioclimatic conditions, especially for those most at risk. In fact, in recent years, due to the ongoing climate changes, the number of heat waves during the summer, in temperate climate regions, has significantly increased. This scenario has an increasing impact on public health and health expenditure. Studies like this can help develop alert systems that give public and health

authorities sufficient time to take a range of targeted actions to reduce the vulnerability of the population.

Author Contributions: Conceptualization, formal analysis, methodology, data curation, writing—original draft preparation P.M. and M.A.R., supervision M.A.R. All authors have read and agreed to the published version of the manuscript.

Funding: This research received no external funding.

Data Availability Statement: Not applicable.

Acknowledgments: The authors are grateful to the anonymous reviewers for their suggestions for improving this manuscript.

Conflicts of Interest: The authors declare no conflict of interest.

Appendix A

Table A1. Annual distribution of the number of days in each TDI class for the provinces of AG, CL, CT, EN, ME, and PA.

Years	Number of Days for Each Class																	
	I st	II nd	III rd	IV th	V th	VI th	I st	II nd	III rd	IV th	V th	VI th	I st	II nd	III rd	IV th	V th	VI th
	AG						CL						CT					
2002	135	18	0	0	0	0	101	47	5	0	0	0	58	42	47	6	0	0
2003	93	60	0	0	0	0	71	73	9	0	0	0	58	28	66	1	0	0
2004	139	14	0	0	0	0	90	61	2	0	0	0	67	56	30	0	0	0
2005	141	12	0	0	0	0	86	63	4	0	0	0	65	64	23	1	0	0
2006	132	21	0	0	0	0	80	64	9	0	0	0	61	58	33	1	0	0
2007	129	24	0	0	0	0	83	56	14	0	0	0	64	56	29	4	0	0
2008	129	24	0	0	0	0	70	76	7	0	0	0	63	52	36	2	0	0
2009	115	38	0	0	0	0	68	78	7	0	0	0	54	57	42	0	0	0
2010	127	26	0	0	0	0	80	59	14	0	0	0	71	48	34	0	0	0
2011	135	18	0	0	0	0	63	78	12	0	0	0	58	56	39	0	0	0
2012	111	42	0	0	0	0	59	70	24	0	0	0	48	53	52	0	0	0
2013	137	16	0	0	0	0	88	61	4	0	0	0	74	45	34	0	0	0
2014	139	14	0	0	0	0	87	66	0	0	0	0	57	70	26	0	0	0
2015	110	43	0	0	0	0	75	66	12	0	0	0	61	48	42	2	0	0
2016	144	9	0	0	0	0	81	71	1	0	0	0	66	55	32	0	0	0
2017	131	22	0	0	0	0	76	64	13	0	0	0	51	56	41	5	0	0
2018	144	9	0	0	0	0	79	70	4	0	0	0	56	63	34	0	0	0
2019	117	36	0	0	0	0	58	84	11	0	0	0	44	48	60	1	0	0
2020	120	33	0	0	0	0	61	76	16	0	0	0	55	57	41	0	0	0
2021	111	42	0	0	0	0	64	62	27	0	0	0	56	33	58	6	0	0
	EN						ME						PA					
2002	153	0	0	0	0	0	75	40	34	3	1	0	70	49	30	4	0	0
2003	153	0	0	0	0	0	65	61	24	3	0	0	63	47	40	3	0	0
2004	153	0	0	0	0	0	86	56	11	0	0	0	76	66	11	0	0	0
2005	153	0	0	0	0	0	99	42	12	0	0	0	81	59	12	1	0	0
2006	153	0	0	0	0	0	84	54	15	0	0	0	72	60	21	0	0	0
2007	152	1	0	0	0	0	90	40	20	3	0	0	75	54	22	2	0	0
2008	153	0	0	0	0	0	76	66	10	1	0	0	66	68	19	0	0	0
2009	153	0	0	0	0	0	83	61	9	0	0	0	71	60	22	0	0	0
2010	153	0	0	0	0	0	89	54	10	0	0	0	82	54	17	0	0	0
2011	153	0	0	0	0	0	93	52	8	0	0	0	77	65	11	0	0	0
2012	153	0	0	0	0	0	68	66	16	3	0	0	63	62	26	2	0	0
2013	153	0	0	0	0	0	97	49	7	0	0	0	84	65	4	0	0	0
2014	153	0	0	0	0	0	95	46	12	0	0	0	83	62	8	0	0	0
2015	153	0	0	0	0	0	77	57	19	0	0	0	72	58	22	1	0	0
2016	153	0	0	0	0	0	95	54	4	0	0	0	87	62	4	0	0	0
2017	153	0	0	0	0	0	83	48	20	2	0	0	78	55	19	1	0	0
2018	153	0	0	0	0	0	94	54	5	0	0	0	74	69	10	0	0	0
2019	153	0	0	0	0	0	71	64	18	0	0	0	60	67	26	0	0	0
2020	153	0	0	0	0	0	80	59	14	0	0	0	64	71	18	0	0	0
2021	121	32	0	0	0	0	79	38	36	0	0	0	61	51	39	2	0	0

Table A2. Annual distribution of the number of days in each TDI class for the provinces of RG, SR, and TP.

Years	Number of Days for Each Class																	
	<i>Ist</i>	<i>IInd</i>	<i>IIIrd</i>	<i>IVth</i>	<i>Vth</i>	<i>VIth</i>	<i>Ist</i>	<i>IInd</i>	<i>IIIrd</i>	<i>IVth</i>	<i>Vth</i>	<i>VIth</i>	<i>Ist</i>	<i>IInd</i>	<i>IIIrd</i>	<i>IVth</i>	<i>Vth</i>	<i>VIth</i>
	RG						SR						TP					
2002	45	58	41	9	0	0	40	43	55	15	0	0	43	53	45	12	0	0
2003	39	34	65	15	0	0	49	23	70	11	0	0	34	34	57	27	1	0
2004	54	63	35	1	0	0	49	49	52	3	0	0	53	43	53	4	0	0
2005	55	70	27	1	0	0	46	60	41	6	0	0	52	64	33	4	0	0
2006	50	45	57	1	0	0	39	52	56	6	0	0	50	50	51	2	0	0
2007	48	54	42	9	0	0	39	54	49	11	0	0	46	54	39	13	1	0
2008	52	30	69	2	0	0	49	22	74	8	0	0	53	25	70	5	0	0
2009	29	60	63	1	0	0	30	52	68	3	0	0	37	53	59	4	0	0
2010	51	55	45	2	0	0	47	43	57	6	0	0	56	47	44	6	0	0
2011	48	52	51	2	0	0	48	52	50	3	0	0	47	51	53	2	0	0
2012	42	36	69	6	0	0	40	39	68	6	0	0	44	34	65	8	2	0
2013	56	46	50	1	0	0	48	48	54	3	0	0	58	40	54	1	0	0
2014	43	63	47	0	0	0	38	52	61	2	0	0	44	64	45	0	0	0
2015	42	43	55	12	1	0	35	45	58	15	0	0	41	45	52	14	1	0
2016	43	49	60	1	0	0	43	43	65	2	0	0	54	50	48	1	0	0
2017	43	44	51	13	2	0	41	35	58	18	1	0	46	50	50	6	1	0
2018	36	54	60	3	0	0	34	48	69	2	0	0	40	62	46	5	0	0
2019	35	39	66	12	1	0	35	33	75	8	2	0	38	36	71	8	0	0
2020	43	39	64	7	0	0	41	37	65	10	0	0	44	48	56	5	0	0
2021	34	35	62	19	3	0	37	31	56	25	4	0	38	40	54	17	4	0

References

- White, P.S.; Jentsch, A. The Search for Generality in Studies of Disturbance and Ecosystem Dynamics. In *Progress in Botany*; Springer: Berlin/Heidelberg, Germany, 2001; pp. 399–450. [\[CrossRef\]](#)
- Pickett, S.T.A.; Kolasa, J.; Armesto, J.J.; Collins, S. The Ecological Concept of Disturbance and Its Expression at Various Hierarchical Levels. *Oikos* **1989**, *54*, 129–136. [\[CrossRef\]](#)
- Yu, R.; Zhai, P. Changes in compound drought and hot extreme events in summer over populated eastern China. *Weather Clim. Extremes* **2020**, *30*, 100295. [\[CrossRef\]](#)
- Páscoa, P.; Gouveia, C.M.; Russo, A.; Ribeiro, A.F.S. Summer hot extremes and antecedent drought conditions in Australia. *Int. J. Clim.* **2022**, *42*, 5487–5502. [\[CrossRef\]](#)
- Beggs, P.J. Impacts of climate change on aeroallergens: Past and future. *Clin. Exp. Allergy* **2004**, *34*, 1507–1513. [\[CrossRef\]](#)
- Bellard, C.; Bertelsmeier, C.; Leadley, P.; Thuiller, W.; Courchamp, F. Impacts of climate change on the future of biodiversity. *Ecol. Lett.* **2012**, *15*, 365–377. [\[CrossRef\]](#)
- Lionello, P.; Abrantes, F.; Gacic, M.; Planton, S.; Trigo, R.; Ulbrich, U. The climate of the Mediterranean region: Research progress and climate change impacts. *Reg. Environ. Chang.* **2014**, *14*, 1679–1684. [\[CrossRef\]](#)
- Segnalini, M.; Bernabucci, U.; Vitali, A.; Nardone, A.; Lacetera, N. Temperature humidity index scenarios in the Mediterranean basin. *Int. J. Biometeorol.* **2013**, *57*, 451–458. [\[CrossRef\]](#)
- Meehl, G.A.; Tebaldi, C. More Intense, More Frequent, and Longer Lasting Heat Waves in the 21st Century. *Science* **2004**, *305*, 994–997. [\[CrossRef\]](#)
- Monforte, P.; Ragusa, M.A. Temperature trend analysis and investigation on a case of variability climate. *Mathematics* **2022**, *10*, 2202. [\[CrossRef\]](#)
- Keellings, D.; Waylen, P. Increased risk of heat waves in Florida: Characterizing changes in bivariate heat wave risk using extreme value analysis. *Appl. Geogr.* **2014**, *46*, 90–97. [\[CrossRef\]](#)
- Cooley, D. Extreme value analysis and the study of climate change. *Clim. Chang.* **2009**, *97*, 77–83. [\[CrossRef\]](#)
- Dosio, A.; Mentaschi, L.; Fischer, E.M.; Wyser, K. Extreme heat waves under 1.5 C and 2 C global warming. *Environ. Res. Lett.* **2018**, *13*, 054006. [\[CrossRef\]](#)
- Wagner, A.P.; McKenzie, E.; Robertson, C.; McMenamin, J.; Reynolds, A.; Murdoch, H. Automated mortality monitoring in Scotland from 2009. *Eurosurveillance* **2013**, *18*, 20451. [\[CrossRef\]](#) [\[PubMed\]](#)
- Burkart, K.; Khan, M.H.; Krämer, A.; Breitner, S.; Schneider, A.; Endlicher, W.R. Seasonal variation of all-cause and cause-specific mortality by age, gender, and socioeconomic condition in urban and rural areas of Bangladesh. *Int. J. Equity Health* **2011**, *10*, 32. [\[CrossRef\]](#) [\[PubMed\]](#)
- Xuan, L.T.; Egondi, T.; Ngoan, L.T.; Toan, T.D.; Huong, L.T. Seasonality in mortality and its relationship to temperature among the older population in Hanoi, Vietnam. *Glob. Health Action* **2014**, *7*, 23115. [\[CrossRef\]](#) [\[PubMed\]](#)
- Seposo, X.T.; Dang, T.N.; Honda, Y. Evaluating the effects of temperature on mortality in Manila city (Philippines) from 2006–2010 using a distributed Lag nonlinear model. *Int. J. Environ. Res. Public Health* **2015**, *12*, 6842–6857. [\[CrossRef\]](#)

18. Schifano, P.; Leone, M.; De Sario, M.; de' Donato, F.; Bargagli, A.M.; D'Ippoliti, D.; Marino, C.; Michelozzi, P. Changes in the effects of heat on mortality among the elderly from 1998–2010: Results from a multicenter time series study in Italy. *Environ. Health* **2012**, *11*, 58. [CrossRef]
19. Sanchis, I.V.; Franco, R.I.; Fernández, P.M.; Zuriaga, P.S.; Torres, J.B.F. Risk of increasing temperature due to climate change on high-speed rail network in Spain. *Transp. Res. Part D Transp. Environ.* **2020**, *82*, 102312. [CrossRef]
20. McCarthy, M.; Armstrong, L.; Armstrong, N. A new heatwave definition for the UK. *Weather* **2019**, *74*, 382–387. [CrossRef]
21. World Meteorological Organization Commission for Climatology. Guidelines on the Definition and Monitoring of Extreme Weather and Climate Events. 2018. Available online: <http://www.wmo.int/pages/prog/wcp/ccl/documents/> (accessed on 1 December 2018).
22. Ebi, K.L.; Kovats, R.S.; Menne, B. An Approach for Assessing Human Health Vulnerability and Public Health Interventions to Adapt to Climate Change. *Environ. Health Perspect.* **2006**, *114*, 1930–1934. [CrossRef]
23. Alonso, L.; Renard, F. A Comparative Study of the Physiological and Socio-Economic Vulnerabilities to Heat Waves of the Population of the Metropolis of Lyon (France) in a Climate Change Context. *Int. J. Environ. Res. Public Health* **2020**, *17*, 1004. [CrossRef] [PubMed]
24. Gamble, J.L.; Balbus, J.; Berger, M.; Bouye, K. *Climate Change and Human Health in Populations of Concern*; U.S. Global Change Research Program: Washington, DC, USA, 2016; ISBN 978-0-16-093241-0. Chapter 9.
25. Schifano, P.; Cappai, G.; De Sario, M.; Michelozzi, P.; Marino, C.; Bargagli, A.M.; Perucci, C. Susceptibility to heat wave-related mortality: A follow-up study of a cohort of elderly in Rome. *Environ. Health* **2009**, *8*, 50. [CrossRef] [PubMed]
26. García, M.C. Thermal differences, comfort/discomfort and Humidex summer climate in Mar del Plata, Argentina. In *Urban Climates in Latin America*; Henríquez, C., Romero, H., Eds.; Springer: Cham, Switzerland, 2019; pp. 83–109.
27. Masterton, J.M.; Richardson, F.A. *Humidex, A Method of Quantifying Human Discomfort Due to Excessive Heat and Humidity*, CLI 1–79, *Environment Canada*; Atmospheric Environment Service: Downsview, ON, Canada, 1979.
28. Lubczyńska, M.J.; Christophi, A.C.; Lelieveld, J. Heat-related cardiovascular mortality risk in Cyprus: A case-crossover study using a distributed lag non-linear model. *Environ. Health* **2015**, *14*, 39. [CrossRef] [PubMed]
29. Astrom, D.O.; Schifano, P.; Asta, F.; Lallo, A.; Michelozzi, P.; Rocklov, J.; Forsberg, B. The effect of heat waves on mortality in susceptible groups: A cohort study of a Mediterranean and a northern European City. *Environ. Health* **2015**, *14*, 30. [CrossRef]
30. De Bono, A.; Peduzzi, P.; Kluser, S.; Giuliani, G. Impacts of summer 2003 heat wave in Europe. *Environ. Alert Bull.* **2004**, *2*, 4. Available online: <https://archive-ouverte.unige.ch/unige:32255> (accessed on 1 March 2004).
31. Conti, S.; Melia, P.; Minelli, G.; Solimini, G.; Toccaceli, V.; Vichi, M.; Beltrano, C.; Perini, L. Epidemiologic study of mortality during the Summer 2003 heat wave in Italy. *Environ. Res.* **2005**, *98*, 390–399. [CrossRef]
32. Mihăilă, D.; Bistricean, P.I.; Lazurca, L.G. Spatial and temporal relevance of some bioclimatic indexes for the study of the bioclimate of Moldova (west of the Prut river). *Globe* **2016**, *48*, 43–329.
33. Rusanescu, C.O.; Rusanescu, M.; Jinescu, C.; Paraschiv, G. Influence of thermal comfort on health. *Rev. Chim.* **2019**, *70*, 1187–1191. [CrossRef]
34. Giorgi, F. Climate change hot-spots. *Geophys. Res. Lett.* **2006**, *33*, 1–4. [CrossRef]
35. Thom, E.C. The discomfort index. *Weatherwise* **1959**, *12*, 57–61. [CrossRef]
36. Stathopoulou, M.I.; Cartalis, C.; Keramitsoglou, I.; Santamouris, M. Thermal remote sensing of Thom's discomfort index (DI): Comparison with in-situ measurements. In Proceedings of the Remote Sensing for Environmental Monitoring, GIS Applications, and Geology V, Bruges, Belgium, 19–22 September 2005; Volume 5983, pp. 131–139.
37. Tselepidaki, I.; Santamouris, M.; Moustiris, C.; Pouloupoulou, G. Analysis of the summer discomfort index in Athens, Greece, for cooling purposes. *Energy Build.* **1992**, *18*, 51–56. [CrossRef]
38. Xu, H.; Hu, X.; Guan, H. Development of a fine-scale discomfort index map and its application in measuring living environments using remotely-sensed thermal infrared imagery. *Energy Build.* **2017**, *150*, 598–607. [CrossRef]
39. Oluwafemi, O.A.; Dombo, T. Geospatial modeling of human thermal comfort in Akure Metropolis using Thom's discomfort index. *Int. J. Environ. Bioenergy* **2019**, *14*, 40–55.
40. Mann, H.B. Nonparametric tests against trend. *Econometrica* **1945**, *13*, 245–259. [CrossRef]
41. Kendall, M.G. *Rank Correlation Methods*; American Psychological Association: Washington, DC, USA, 1948.
42. Simonetti, A.D.A.; Marazzi, M.C. Birth rate, death rate and aging of the Italian population in the last 25 years. *Nuovi Ann. d'Igiene Microbiol.* **1978**, *29*, 421–441.
43. Mazdiyasi, O.; AghaKouchak, A.; Davis, S.J.; Madadgar, S.; Mehran, A.; Ragno, E.; Sadegh, M.; Sengupta, A.; Ghosh, S.; Dhanya, C.T.; et al. Increasing probability of mortality during Indian heat waves. *Sci. Adv.* **2017**, *3*, e1700066. [CrossRef]
44. Fratianni, S.; Acquattrota, F. The Climate of Italy. In *Landscapes and Landforms of Italy, World Geomorphological Landscape, Soldati—Marchetti Editors*; Springer: Berlin/Heidelberg, Germany, 2017; pp. 29–38.
45. Pinna, M. Contributi di climatologia. *Mem. Soc. Geogr. Ital. Roma* **1985**, *39*, 169–194.
46. Guarino, R.; Pasta, S. Sicily: The island that didn't know to be an archipelago. *Ber. Reinhold TÜXen Ges.* **2018**, *30*, 133–148.
47. Thom, H.C.S. *Some Methods of Climatological Analysis*; World Meteorological Organization: Geneva, Switzerland, 1966; note n. 81.
48. Giles, B.D.; Balafoutis, C.; Maheras, P. Too hot for comfort: The heatwaves in Greece in 1987 and 1988. *Int. J. Biometeorol.* **1990**, *34*, 98–104. [CrossRef]

49. Mavrakis, A.; Spanou, A.; Pantavou, K.; Katavoutas, G.; Theoharatos, G.; Christides, A.; Verouti, E. Biometeorological and air quality assessment in an industrialized area of eastern Mediterranean: The Thriassion Plain, Greece. *Int. J. Biometeorol.* **2012**, *56*, 737–747. [[CrossRef](#)]
50. Staiger, H.; Laschewski, G.; Grätz, A. The perceived temperature—A versatile index for the assessment of the human thermal environment. Part A: Scientific basics. *Int. J. Biometeorol.* **2012**, *56*, 165–176. [[CrossRef](#)] [[PubMed](#)]
51. Monforte, P.; Ragusa, M.A. Evaluation of the air pollution in a Mediterranean region by the air quality index. *Environ. Monit. Assess.* **2018**, *190*, 625. [[CrossRef](#)] [[PubMed](#)]
52. Yusuf, A.S.; Edet, C.O.; Oche, C.O.; Agbo, E.P. Trend analysis of temperature in Gombe state using Mann Kendall trend test. *J. Sci. Res. Rep.* **2018**, *20*, 1–9.
53. Yadav, R.; Tripathi, S.K.; Pranuthi, G.; Dubey, S.K. Trend analysis by Mann-Kendall test for precipitation and temperature for thirteen districts of Uttarakhand. *J. Agrometeorol.* **2014**, *16*, 164. [[CrossRef](#)]
54. Fallah Ghalhar, G.; Farhang Dehghan, S.; Asghari, M. Trend analysis of humidex as a heat discomfort index using Mann-Kendall and Sen's slope estimator statistical tests. *Environ. Health Eng. Manag.* **2022**, *9*, 165–176. [[CrossRef](#)]
55. Robaa, E.-S.M.; Al-Barazanji, Z. Mann-Kendall trend analysis of surface air temperatures and rainfall in Iraq. *Q. J. Hung. Meteorol. Serv.* **2015**, *119*, 493–514.
56. Modarres, R.; da Silva, V.d.P.R. Rainfall trends in arid and semi-arid regions of Iran. *J. Arid Environ.* **2007**, *70*, 344–355. [[CrossRef](#)]
57. Famoso, F.; Lanzafame, R.; Monforte, P.; Oliveri, C.; Scandura, P.F. Air quality data for Catania: Analysis and investigation case study 2012–2013. *Energy Procedia* **2015**, *81*, 644–654. [[CrossRef](#)]
58. Partal, T.; Kahya, E. Trend analysis in Turkish precipitation data. *Hydrol. Process. Int. J.* **2006**, *20*, 2011–2026. [[CrossRef](#)]
59. Hipel, K.W.; McLeod, A.I. *Time Series Modelling of Water Resources and Environmental Systems*; Elsevier: Amsterdam, The Netherlands, 1994; ISBN 9780080870366.
60. *Managing the Risks of Extreme Events and Disasters to Advance Climate Change Adaptation: Special Report of the Intergovernmental Panel on Climate Change*; Field, C.B.; Barros, V.; Stocker, T.F.; Dahe, Q. (Eds.) Cambridge University Press: New York, NY, USA, 2012.
61. Kambezidis, H.D.; Psiloglou, B.E.; Varotsos, K.V.; Giannakopoulos, C. Climate Change and Thermal Comfort in Greece. *Climate* **2021**, *9*, 10. [[CrossRef](#)]
62. Infusino, E.; Caloiero, T.; Fusto, F.; Calderaro, G.; Brutto, A.; Tagarelli, G. Characterization of the 2017 Summer Heat Waves and Their Effects on the Population of an Area of Southern Italy. *Int. J. Environ. Res. Public Health* **2021**, *18*, 970. [[CrossRef](#)] [[PubMed](#)]